Guiding AMR Parsing with Reverse Graph Linearization

Anonymous ACL submission

Abstract

Abstract Meaning Representation (AMR) parsing aims to extract an abstract semantic graph from a given sentence. The sequence-to-sequence approaches, which linearize the semantic graph into a sequence of nodes and edges and generate the linearized graph directly, have achieved good performance. However, we observed that these approaches suffer from structure loss accumulation during the decoding process, leading to a much lower F1-score for nodes and edges decoded later compared to those decoded earlier. To address this issue, we propose a novel Reverse Graph Linearization (RGL) enhanced framework. RGL defines both default and reverse linearization orders of an AMR graph, where most structures at the back part of the default order appear at the front part of the reversed order and vice versa. RGL incorporates the reversed linearization to the original AMR parser through a two-pass self-distillation mechanism, which guides the model when generating the default linearizations. Our analysis shows that our proposed method significantly mitigates the problem of structure loss accumulation, outperforming the previously best AMR parsing model by 0.8 and 0.5 Smatch scores on the AMR 2.0 and AMR 3.0 dataset, respectively. We will release the code and models for reproduction.

1 Introduction

Abstract Meaning Representation (AMR) (Banarescu et al., 2013) is a formalization of a sentence's meaning using a directed acyclic graph that abstracts away from shallow syntactic features and captures the core semantics of the sentence. AMR parsing involves transforming a textual input into its AMR graph, as illustrated in Figure 1. Recently, sequence-to-sequence (seq2seq) based AMR parsing models (Xu et al., 2020b; Bevilacqua et al., 2021; Wang et al., 2021; Bai et al., 2022; Yu and Gildea, 2022b; Chen et al., 2022; Cheng et al., 2022) have significantly improved the performance of AMR parsing. In these models, the AMR graph is first linearized into a token sequence during traditional seq2seq training, and the output sequence is then restored to the graph structure after decoding. AMR parsing has proven beneficial for many NLP tasks, such as summarization (Liao et al., 2018; Hardy and Vlachos, 2018), question answering (Mitra and Baral, 2016; Sachan and Xing, 2016), dialogue systems (Bonial et al., 2020; Bai et al., 2021), and information extraction (Rao et al., 2017; Wang et al., 2017; Zhang and Ji, 2021; Xu et al., 2022).

In this study, we address the issue of structure loss accumulation in seq2seq-based AMR parsing. Our analysis (Figure 2) shows that the F1-score of

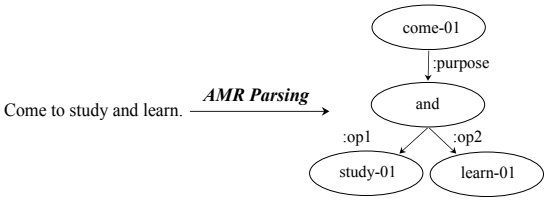

Figure 1: An example of AMR Parsing of the sentence "Come to study and learn".

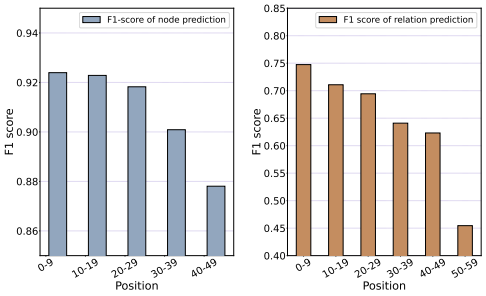

(a) Node prediction (b) Relation prediction

Figure 2: There is a negative correlation between the F1-score of the node or relation prediction and the position. The results are obtained from AMRBART (Bai et al., 2022) on the test set of AMR 2.0.

structure prediction (node and relation) decreases as the generation direction progresses. This phenomenon is a consequence of the error accumulation in the auto-regressive decoding process, a common problem in natural language generation (Ing, 2007; Zhang et al., 2019c; Liu et al., 2021).

However, unlike natural language, the linearization of AMR graphs does not follow a strict order, as long as the sequence preserves all nodes and relations in the AMR graph. To this end, we define two linearization orders based on the depth-first search (DFS) traversal, namely Left-to-Right (L2R) and Right-to-Left (R2L). The L2R order is the conventional linearization used in most previous works (Bevilacqua et al., 2021; Bai et al., 2022; Chen et al., 2022), where the leftmost child corresponding to the penman annotation is traversed first. In contrast, the R2L order is its reverse, where the structures at the end of the L2R order appear at the beginning of the R2L order. By training AMR parsing models with R2L linearization, it improves the accuracy of predictions for the structures at the end of the L2R order, which are less affected by the accumulation of structure loss.

We propose to enhance AMR parsing with reverse graph linearization (RGL). Specifically, we incorporate an additional encoder to integrate the reverse linearization graph and replace the original transformer decoder with a mixed decoder that utilizes gated dual cross-attention, taking input from both the hidden states of the sentence encoder and the graph encoder. We design a two-pass self-distillation mechanism to prevent the model from overfitting to the gold reverse linearized graph as well as to further utilize it to guide the model training. Our analysis shows that our proposed method significantly mitigates the problem of structure loss accumulation, outperforming the previously best AMR parsing model (Bai et al., 2022) by 0.8 Smatch score on the AMR 2.0 dataset and 0.5 Smatch score on the AMR 3.0 dataset.

Our contributions can be listed as follows:

1. We explore the structure loss accumulation problem in sequence-to-sequence AMR parsing.

2. We propose a novel RGL framework to alleviate the structure loss accumulation by incorporating reverse graph linearization into the model.

3. The RGL outperforms the previous best AMR parser by 0.8 and 0.5 smatch scores on AMR 2.0 and AMR 3.0, which demonstrates the effectiveness and superiority of our proposed method.

Direction	Linearized AMR Graph
Left-to-Right	(c/come-01 :purpose (a/and :op1 (s/study-01) :op2 (l/learn-01)))
Right-to-Left	(c/come-01 :purpose (a/and :op2 (l/learn-01) :op1 (s/study-01)))

Table 1: The AMR graph shown in Figure 1 with different linearization order. "Left-to-Right" follows the standard DFS traversal order. "Right-to-Left" follows the reverse DFS traversal order.

2 Backgrounds

2.1 Seq2Seq based AMR Parsing

In our work, we followed previous methods (Ge et al., 2019; Bevilacqua et al., 2021; Bai et al., 2022), which formulate AMR parsing as a sequence-to-sequence generation problem. Formally, given a sentence $\mathbf{x} = (x_1, x_2, ..., x_N)$, the model needs to generate a linearized AMR graph $\mathbf{y} = (y_1, y_2, ..., y_M)$ in an auto-regressive manner.

Assuming that we have a training set containing data with N sentence-linearized graph pairs (x_i, y_i), the total training loss of the model is computed by the cross-entropy loss which is listed as follows:

$$L_{CE} = -\sum_{i=1}^{N}\sum_{t=1}^{m_i} logp(y_t^i | y_{<t}^i, x_i) \quad (1)$$

where m_i is the length of i^{th} linearized AMR graph.

After obtaining the linearized AMR graph, which is a sequence generated by the model, We post-process the sequence with rules to restore it to an AMR graph.

2.2 Graph Linearization Order

As shown in Table 1, we formalize two types of graph linearization, the corresponding AMR graph is shown in Figure 1. **Left-to-Right (L2R)** denotes that when we use the depth-first search (DFS) to traverse the children of a node, we first start from the leftmost child and then traverse to the right, which is identical to the order of penman annotation and is the default order of sequence-to-sequence based AMR parsers (Bevilacqua et al., 2021; Bai et al., 2022; Chen et al., 2022). In contrast, **Right-to-Left (R2L)** traverses from the rightmost child to the leftmost child, which is the reverse of the standard traversal order. When the input sentence is long or contains multi-sentence, the nodes or relationships that are positioned later in the L2R sequence will appear earlier in the R2L sequence.

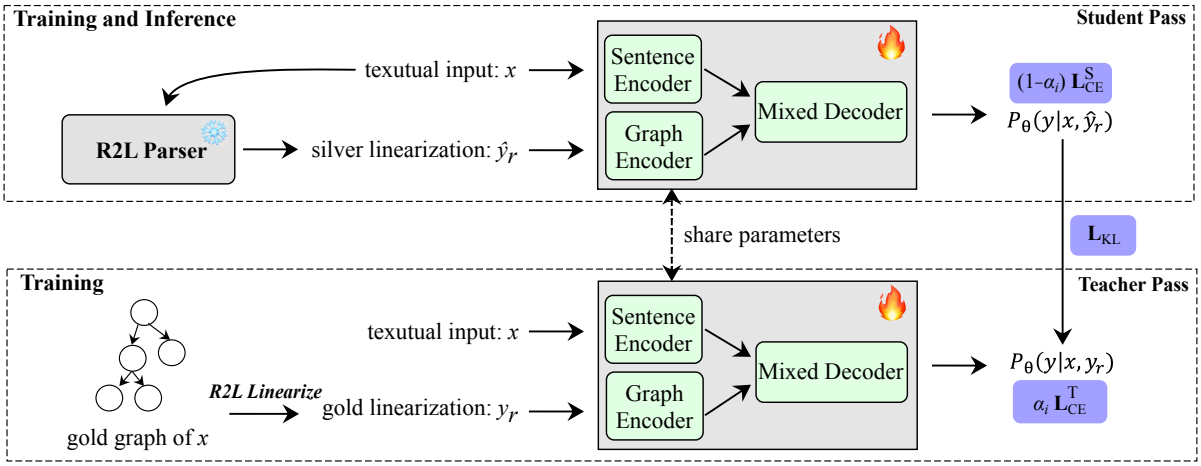

Figure 3: The overview of our method. In addition to the encoder-decoder model, an additional graph encoder is used to incorporate reverse graph linearization. Following the paradigm of self-distillation, we regard the model with the input of the gold linearization y_r and x as the teacher model and $\hat{y}_r$ parsed by a pre-trained R2L parser and x as the student model. The model does twice forward pass to obtain the output probabilities of the teacher and the student in each training step. We calculate the cross-entropy loss of teacher and student as well as their KL divergence as the training loss. Given a sentence x during inference, the model generates the standard AMR linearization using x and its silver linearization $\hat{y}_r$.

3 Methodology

3.1 Overview

Our method is illustrated in Figure 3. In addition to the traditional encoder-decoder architecture, we have incorporated a graph encoder to include the reverse linearization sequence. As a result, the model now takes both the sentence and its reverse linearization as input. We modify the original transformer decoder with a mixed decoder that uses gated dual cross-attention in each decoder layer, allowing the integration of hidden representations from both the sentence encoder and the graph encoder. During inference, we need an additional R2L AMR parser that generates the reverse linearization $\hat{y}_r$ of the sentence and then feed both the input sentence x and $\hat{y}_r$ to the model.

To obtain reverse linearization during training, a common intuitive approach is to linearize the gold AMR graph into the gold reverse linearization, denoted by y_r. However, simply using y_r and the source sentence x as input for all training data can lead to overfitting of the model to y_r, causing it to ignore the importance of the source sentence. As a result, the model may simply copy from y_r and generate y during training. This can limit the model's performance during inference due to the noise introduced by the generated reverse linearization, denoted by $\hat{y}_r$.

To prevent the model from overfitting to y_r we introduce silver linearization $\hat{y}_r$ during training. While we still hope to utilize the gold linearization y_r to guide the training, we design a two-pass self-distillation mechanism. Alongside y_r, we incorporate $\hat{y}_r$, which is parsed by the additional R2L AMR parser during training. The teacher model takes y_r and x as input, while the student model takes $\hat{y}_r$ and x. During each training step, the model performs two forward passes and computes cross-entropy losses, L_{CE}^T for the teacher and L_{CE}^S for the student. We employ KL divergence L_{KL} to guide the student with the teacher's output. We also design a loss scheduler to balance the weight α_i for L_{CE}^T and L_{CE}^S at optimization step i.

3.2 Model Structure

As shown in Figure 3, our model mainly consists of three parts: sentence encoder, graph encoder, and mixed decoder. The major structural difference from standard pretrained models, e.g. BART (Lewis et al., 2020), is that we use a graph encoder to integrate the reverse linearized structural information to guide the model.

Sentence Encoder The sentence encoder receives the given sentence $s = (s_1, s_2, ..., s_N)$, and encodes it to the hidden representations $H^s = (\mathbf{h}_1^s, \mathbf{h}_2^s, ..., \mathbf{h}_N^s)$, which is the same as the encoder of pretrained transformer models.

Graph Encoder Following (Bevilacqua et al., 2021; Bai et al., 2022), we adopt the standard transformer encoder to encode the structural information. Given the reverse-linearized AMR graph, the output of the graph encoder is $H^g = (\mathbf{h}_1^g, \mathbf{h}_2^g, ..., \mathbf{h}_M^g)$.

Mixed Decoder Different from the traditional decoder, the mixed decoder takes the hidden states of the sentence H^s and the graph H^g via a gated dual cross-attention layer as shown in Figure 4. The gated dual cross-attention layer contains two cross-attention modules which are used to integrate H^s and H^g respectively. In the decoder layer, the output of the self-attention module is $S^z \in \mathbb{R}^{k\times d}$, where k is the number of tokens in the decoder input and d is the size of the hidden state. The output of each cross-attention module can be computed as:

$$S^s = \text{CrossAttn}^s(S^z, H^s, H^s) \quad (2)$$

$$S^g = \text{CrossAttn}^g(S^z, H^g, H^g) \quad (3)$$

where the two cross-attention modules contains the same query S^z but different key-value H^s and H^g respectively.

The output of the gated dual cross-attention module S^o is the weighted sum of S^s and S^g.

$$S^o = \mathbf{g} \cdot S^g + (\mathbf{1} - \mathbf{g}) \cdot S^s$$

where $\mathbf{g} \in \mathbb{R}^{K\times 1}$ is predicted by a feed-forward network:

$$\mathbf{g} = \sigma(\mathbf{V}^{\mathrm{T}}\tanh(\mathbf{W}^{\mathrm{T}}S^z + b_1) + b_2) \quad (4)$$

σ is the sigmoid function, $\mathbf{W} \in \mathbb{R}^{d\times d}$, $\mathbf{V} \in \mathbb{R}^{d\times 1}$, $b_1 \in \mathbb{R}^{d\times 1}$ and $b_2 \in \mathbb{R}$ are trainable parameters and bias.

3.3 Training Objective

The training objective of the RGL is:

$$L = \alpha_i L_{CE}^T + (1 - \alpha_i)L_{CE}^S + L_{KL} \quad (5)$$

where α_i is a balancing weight related to i_{th} iteration. L_{CE}^T and L_{CE}^S are the cross-entropy loss of the teacher and the student respectively and L_{KL} is the self-distillation loss.

Self-distillation To further guide the model with gold reverse linearization y_r during training as well as to avoid the model from overfitting to it and ignoring the sentence x, we propose a two-pass self-distillation mechanism during training. As shown in equation 6 and 7, we regard the forward pass taking y_r as input a teacher and $\hat{y}_r$ as a student. To obtain the output distribution of both the teacher and the student, the model performs two forward passes in one training step. Note that the teacher and the student model share the same parameters.

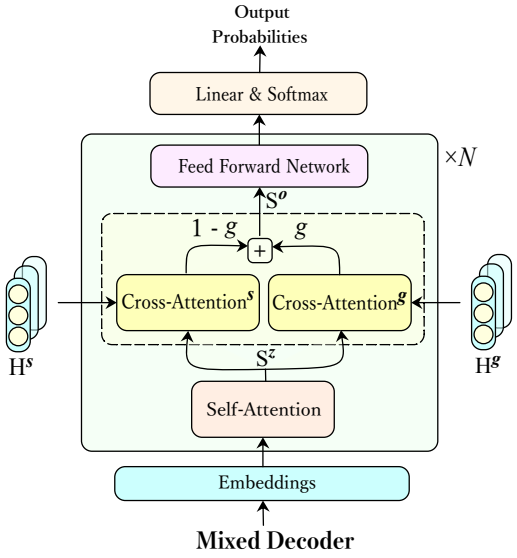

Figure 4: The illustration of the mixed decoder in RGL. H^s and H^g are the hidden representations from the sentence encoder and graph encoder. The module enclosed by the dashed line is the gated dual cross-attention, which integrates the outputs of the dual attention through a gate predicted by an FFN. For brevity and focus, the residual connection and normalization are omitted from the figure.

$$p(y|x, y_r) = \prod_{i=1}^{M} p(y_i|(y_1, y_2, ..., y_{i-1}), x, y_r) \quad (6)$$

$$q(y|x, \hat{y_r}) = \prod_{i=1}^{M} p(y_i|(y_1, y_2, ..., y_{i-1}), x, \hat{y_r}) \quad (7)$$

To distill the knowledge from the teacher pass to the student pass, we guide the output of student pass with the teachers by minimizing the Kullback–Leibler divergence loss:

$$L_{KL}(p, q) = \sum_{i=1}^{D} p_i log(\frac{p_i}{q_i}) \quad (8)$$

where p and q are the output probabilities of the teacher and the student respectively, D is the number of classes which is the total size of the target vocabulary.

Loss scheduler Inspired by the idea of curriculum learning, we introduce a loss scheduler to better balance the training process. We set an adaptive

coefficient α_i to control the weights of L_{CE}^T and L_{CE}^S. α_i gradually decays with the increase of training step i. The model is supposed to learn more from gold linearization when its capability is weak so that the model can converge quickly. When the model's capability is strong, it is supposed to have the ability to infer from the noisy silver linearization, which can make the model more capable and robust to noise during inference since we do not have a gold linearization graph during inference. The α_i can be computed as exponential decay:

$$\alpha_i = k_1 * e^{-k_2 * i}, 0 \leq i \leq total\_steps \quad (9)$$

where k_1 and k_2 are hyper-parameters that can control the upper- and lower-bounds of the α_i. We set the upper bound of α_i to 0.8 and the lower bound to 0.2 without further tuning.

3.4 Inference

Given a sentence, we first use the R2L AMR parser to generate its reverse linearization. Then the trained RGL model takes the reverse linearization and the sentence as input and decodes the standard L2R AMR linearization.

4 Experiments

To demonstrate the effectiveness of the proposed method, we conduct a set of experiments to assess its performance with respect to State-of-the-Art models. We first present the detailed information of datasets (Subsection 4.1) and evaluation metrics (Subsection 4.2) and models (Subsection 4.3) used in our experiments.

4.1 Datasets

We conducted our experiments on two AMR benchmark datasets, AMR 2.0 and AMR 3.0. AMR 2.0 contains 36521, 1368, and 1371 sentence-AMR pairs in training, validation, and testing sets, respectively. AMR 3.0 has 55635, 1722, and 1898 sentence-AMR pairs for training validation and testing set, respectively.

4.2 Evaluation Metrics

We use the Smatch scores (Cai and Knight, 2013) and further the fine-grained scores (Damonte et al., 2017) to evaluate the performance. The detailed explanations of the evaluation metric are shown in Appendix B.

BLINK (Wu et al., 2019) is used to add wiki tags to the predicted AMR graphs in all the systems in our experiments. We do not apply any re-category methods and other post-processing methods are the same with Bai et al. (2022) to restore AMR from the token sequence.

4.3 Compared Systems

AMRBART We use the current state-of-the-art sequence-to-sequence AMR Parser proposed by (Bai et al., 2022) as our main baseline model.

AMRBART+multitask A simple method to integrate extra linearization order is through multitask learning, where the model learns to predict both the L2R and R2L AMR graph. During training, a task identifier <L2R> or <R2L> is added to the beginning of the input sentence to differentiate the output's order. During inference, we individually test the two orders and select the order with the higher Smatch score (L2R) as the final result.

RGL The proposed method as in Section 3. We initialize our model using AMRBART (Bai et al., 2022). Note that the sentence encoder and the graph encoder are initialized the same as the AMRBART encoder, but they have individual gradients during training.

As for the R2L parser for inference, we fine-tune AMRBART (Bai et al., 2022) using sentences and their corresponding reverse linearized AMR graphs of the training sets.

During training, we also need an R2L parser to parse the sentence into the silver graph of the total training set. If we use the R2L parser exactly the same as that in inference, it will generate silver graphs that are almost the same as the gold graphs, because the R2L parser has already seen all of these data during training. To solve this problem, we use 30% of the training set (10000 samples in AMR 2.0, 15000 samples in AMR 3.0) to train a "weaker" R2L parser, and then use it to infer the entire training set to obtain the silver linearizations during training.

Full training details of the compared systems are listed in Appendix A.

4.4 Main Results

We report the results of our method with several Seq2seq baselines on two major datasets, AMR 2.0 and AMR 3.0 in table 2. Our method outperforms previous methods significantly and provides a state-of-the-art AMR parser.

	Model	SMATCH	NoWSD	Wiki	Conc.	NER	Neg.	Unll.	Reen.	SRL
AMR 2.0	Cai and Lam (2020)	78.7	79.2	81.3	88.1	87.1	66.1	81.5	63.8	74.5
	Zhou et al. (2021)	81.8	82.3	78.8	88.7	88.5	69.7	85.5	71.1	80.8
	SPRING (Bevilacqua et al., 2021)	83.8	84.4	84.3	90.2	90.6	74.4	86.1	70.8	79.6
	SPRING (w/ silver) (Bevilacqua et al., 2021)	84.3	84.8	83.1	90.8	90.5	73.6	86.7	72.4	80.5
	ATP (Chen et al., 2022)	85.2	85.6	84.2	90.7	**93.1**	74.9	88.3	74.7	**83.3**
	AMRBART (Bai et al., 2022)	85.4	85.8	81.4	91.2	91.5	74.0	88.3	73.5	81.5
	AMRBART (ours)	85.3	85.7	84.0	91.2	90.8	74.3	88.2	73.2	81.3
	AMRBART+Multitask (ours)	85.8	86.2	83.9	91.4	91.2	75.7	88.6	74.3	81.9
	RGL (ours)	**86.1**	**86.4**	**84.5**	**91.5**	91.7	**76.1**	**88.9**	**74.8**	82.1
AMR 3.0	SPRING (w/ silver) (Bevilacqua et al., 2021)	83.0	83.5	82.7	89.8	87.2	73.0	85.4	70.4	78.9
	ATP (Chen et al., 2022)	83.9	84.3	81.0	89.7	88.4	**73.9**	87.0	**73.9**	**82.5**
	AMRBART (Bai et al., 2022)	84.2	84.6	78.9	90.2	**88.5**	72.1	87.1	72.4	80.3
	AMRBART (ours)	84.2	84.6	**83.3**	90.1	88.2	73.2	87.1	71.9	80.0
	AMRBART+Multitask (ours)	84.4	84.7	82.9	90.3	88.1	73.1	87.3	72.9	80.4
	RGL (ours)	**84.7**	**85.1**	82.8	**90.5**	88.2	72.3	**87.5**	73.2	80.8

Table 2: SMATCH and fine-grained F1 scores on AMR 2.0 and 3.0. RGL outperforms AMRBART(ours) significantly with $p < 0.001$ for both AMR 2.0 and AMR 3.0.

Model	SMATCH
AMRBART (Ours)	85.3
RGL **w/ R2L** (Ours)	86.1
RGL **w/ L2R** (Ours)	85.8

Table 3: Effect of the different linearization orders to the model. "RGL **w/ R2L**" is the RGL model where we feed the reverse graph linearization as the extra input. "RGL **w/ L2R**" is the control group where we feed the standard L2R linearization to the graph encoder of the model without changing other conditions.

Model	SMATCH
AMRBART (Ours)	85.3
RGL (ours)	**86.1**
- w/o silver linearization	85.0
- w/o loss scheduler	85.9
- w/o self-distillation	85.7

Table 4: Ablation study results on the RGL. "w/o loss scheduler": remove the loss scheduler in the training process, where we simply add up all loss terms. "w/o self-distillation": remove the L_{KL} and L_{CE}^{T} from training objective. "w/o silver linearization": remove the L_{KL} and L_{CE}^{S} from training objective.

In comparison with the baseline AMRBART, our method outperforms it by **0.8** Smatch point on AMR 2.0 and **0.5** Smatch point on AMR 3.0. Moreover, our method does not introduce any additional data and is compatible with existing methods such as (Chen et al., 2022) and (Bai et al., 2022).

The multitask learning method also leads to significant improvement, which also proves the effectiveness of incorporating the reverse order to AMR parsing. Our proposed RGL outperforms the multitask in both AMR 2.0 and AMR 3.0, which demonstrates the superiority of our method.

4.5 Effect of reverse linearization

To further demonstrate the role played by the reverse graph linearization in the RGL model, we replaced the reverse linearization with the standard linearization without changing other conditions. Then we conduct our experiment on the AMR 2.0 dataset. Experiment results are shown in table 3.

As shown in table 3, the performance of the model degrades when the extra input of the model becomes the standard left-to-right AMR graph, which proves the effectiveness of incorporating the reverse linearization. However, the performance of RGL with standard linearization is still improved compared to AMRBART, which may be due to the effect of self-distillation. self-distillation provides the ground truth as the model input during the training and forces the model to predict the same distribution when it is faced with noisy input. We suppose that this may improve the robustness of the model at inference. The results of this experiment are consistent with the experimental conclusions of the ablation study in Section 4.6, where self-distillation itself can bring help to the model.

4.6 Ablation Study

Table 4 presents the results of an ablation study in which we analyze how different training methods affect the performance of RGL.

We observed a significant drop in model performance when we removed the silver linearization from the training process. This approach involves

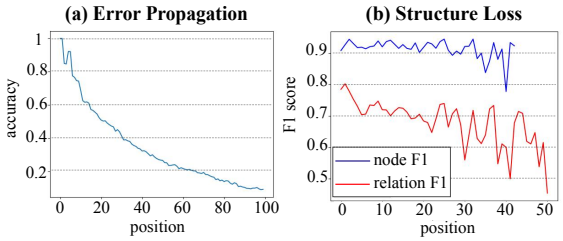

Figure 5: The descent of (a) position-wise accuracy and (b) graph-wise F1-score of nodes and relations as the decoding progresses. The results are from AMRBART (Bai et al., 2022) on the test set of AMR 2.0.

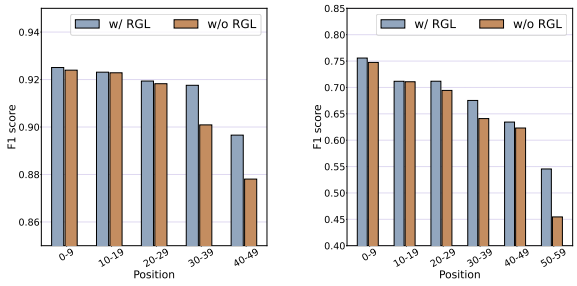

(a) Node prediction (b) Relation prediction

Figure 6: F1-score of nodes and relations with the increase of the predicted length of AMRBART (Bai et al., 2022) represented by blue bars and RGL represented by orange bars.

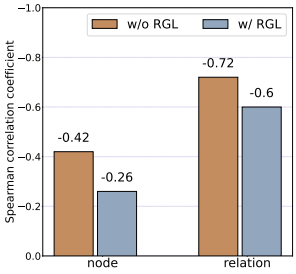

Figure 7: Spearman correlation coefficients between the F1 score and prediction positions of AMRBART and RGL. A higher bar indicates a stronger relationship between the performance of the node or relationship prediction and the prediction position, indicating that the model is more influenced by the structure loss.

feeding the model with the gold linearization during training while using the silver linearization at inference. We believe this drop in performance occurred for two reasons. First, since the gold reverse linearization and the target are highly similar in structure, the model can be easily overfitted to the gold reverse linearization and ignore the source sentence. This can cause the model to simply replicate the input y_r to y instead of accurately parsing the sentence to an AMR graph. Second, the lack of a structure loss for the gold AMR sequence during training means that the model does not learn to differentiate the correct part of the graph from the noisy part, which is required during inference. Therefore, without the silver graph during training, our model cannot be effectively trained.

We also observed a significant drop in performance when we removed self-distillation from the training process. This highlights the importance of self-distillation in our method, which helps the model avoid the error information caused by noise in silver graphs during training. Nevertheless, our method still outperformed AMRBART, even without self-distillation, which demonstrates the effectiveness of incorporating the reverse linearization into AMR parsing.

Finally, when we removed the loss scheduler, the performance of the model degraded. This emphasizes the importance of the loss scheduler in balancing the teacher and the student during training and enhancing the performance of our method.

5 Analysis

5.1 Error propagation vs. structure loss

Figure 5 highlights the distinction between error propagation and structure loss. Error propagation is typically evaluated position-wise or within a limited window (Liu et al., 2021), and is observed in almost every autoregressive method, including sequence-to-sequence based AMR parsing. Once a previous prediction is misplaced or incorrect, subsequent predictions tend to follow the same pattern. In contrast, structure loss evaluates the validity of a node or relation based on its existence in the entire gold graph, rather than its position or window. We argue that structure loss provides a more accurate reflection of the challenges in AMR parsing and other structure generation tasks because it measures the overall quality of the generated AMR graph.

5.2 Effect of RGL on structure loss

The decrease of F1 scores for nodes and relations with prediction length is shown in Figure 6. Compared with the baseline AMRBART, there is a significant improvement in the F1 score of both the node and relation prediction of the RGL when the prediction length is greater than 30.

To quantify the results, we measured the Pearson coefficients between the F1 scores of nodes

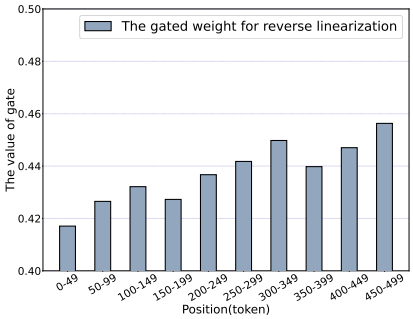

Figure 8: The histogram of the gated weight in the gated dual cross-attention with the increase of the position during inference. A higher value indicates that the model is attending more to the output of the reverse graph encoder in the cross-attention layer. We divided the positions into buckets of size 50 and computed the average gate value across all positions and layers within each bucket, represented by the blue bar in the diagram.

and relations and the prediction length, which is shown in Figure 7. Compared to AMRBART, the Pearson correlation coefficient of node F1 scores with prediction position decreased from -0.42 to -0.26. The coefficient of relation F1 scores with prediction position decreased from -0.72 to -0.6. The results above prove that the RGL model can indeed alleviate the structure loss problem.

Our analysis also reveals that node prediction is less affected by structure loss accumulation than relation prediction. We believe this is mainly because node prediction in AMR parsing is relatively easier, whereas relation prediction requires correct node predictions as a precondition.

5.3 Balancing source and reverse linearization

Figure 8 shows the results of a quantitative analysis of the weight g in the gated dual cross-attention of RGL. We recorded the positions and gated values during model inference on the validation set[1] .

The diagram reveals that the average value of the gate is less than 0.5, indicating that the model pays more attention to the source sentence than to the reverse linearization. This suggests that the model is performing sentence-to-AMR conversion, rather than simply copying the reverse linearization.

Furthermore, there is a positive correlation between the gated weight and the position, which provides insight into how our method works. In positions closer to the beginning, the model has greater confidence, resulting in smaller structure loss. The model can predict the AMR graph using only the original source sentence. As the position increases, the model needs to refer to the reverse linearization to compensate for the accumulation of structure loss. Consequently, the gated weight for the reverse linearization becomes larger as the position increases.

[1]The value range of the x-axis is significantly longer than that of Figure 2 because we count all the output tokens in this experiment, instead of picking out tokens representing nodes and relationships from all tokens.

6 Related Work

AMR parsing aims to convert a textual input to an AMR semantic graph (Banarescu et al., 2013). There are mainly four AMR Parsing strategies in previous work, two-stage approaches (Flanigan et al., 2014; Lyu and Titov, 2018; Zhang et al., 2019a; Zhou et al., 2020), graph-based approaches (Zhang et al., 2019b; Cai and Lam, 2020), transition-based approaches (Naseem et al., 2019; Lee et al., 2020; Fernandez Astudillo et al., 2020; Zhou et al., 2021), sequence-to-sequence approaches (Ge et al., 2019; Xu et al., 2020a; Bevilacqua et al., 2021; Wang et al., 2021; Bai et al., 2022; Chen et al., 2022; Yu and Gildea, 2022b; Cheng et al., 2022). In terms of AMR graph linearization, Bevilacqua et al. (2021) explores which linearization method is better for AMR parsing, and Chen et al. (2022) studied how to linearize different semantic resources like SRL to enhance AMR parsing. Some methods have also been proposed to incorporate graph information into sequence-to-sequence models to compensate for the discrepancy between graph and sequence (Yu and Gildea, 2022a; Bai et al., 2022). While previous seq2seq-based AMR parsing models mostly take the L2R linearization order by default, our work first explores how to leverage different graph linearization orders to enhance AMR parsing.

7 Conclusion

In this work, we propose a novel Reverse Graph Linearization (RGL) enhanced framework to address the structure loss accumulation problem observed in the seq2seq-based AMR parsing. Through extensive experiments and analysis, it shows that RGL significantly mitigates the problem of structure loss accumulation and outperforms the previous state-of-the-art model on both AMR 2.0 and AMR 3.0 datasets, which demonstrates the effectiveness of the proposed approach.

8 Limitation

Compared to traditional sequence-to-sequence AMR parser, our model needs an additional R2L parser to generate the reverse linearizations, although it can be easily obtained by fine-tuning off-the-shelf AMR parser, e.g. AMRBART (Bai et al., 2022) and SPRING (Bevilacqua et al., 2021). Due to the necessity to generate the reverse linearization before AMR parsing, the inference is two times slower than the one-pass AMR parser.

9 Ethics Consideration

We collect our data from public datasets that permit academic use and buy the license for the datasets that are not free. The open-source tools we use for training and evaluation are freely accessible online without copyright conflicts.

References

Xuefeng Bai, Yulong Chen, Linfeng Song, and Yue Zhang. 2021. Semantic representation for dialogue modeling. *ArXiv*, abs/2105.10188.

Xuefeng Bai, Yulong Chen, and Yue Zhang. 2022. Graph pre-training for AMR parsing and generation. In *Proceedings of the 60th Annual Meeting of the Association for Computational Linguistics (Volume 1: Long Papers)*, pages 6001–6015, Dublin, Ireland. Association for Computational Linguistics.

Laura Banarescu, Claire Bonial, Shu Cai, Madalina Georgescu, Kira Griffitt, Ulf Hermjakob, Kevin Knight, Philipp Koehn, Martha Palmer, and Nathan Schneider. 2013. Abstract meaning representation for sembanking. In *Proceedings of the 7th linguistic annotation workshop and interoperability with discourse*, pages 178–186.

Michele Bevilacqua, Rexhina Blloshmi, and Roberto Navigli. 2021. One spring to rule them both: Symmetric amr semantic parsing and generation without a complex pipeline. In *Proceedings of the Thirty-Fifth AAAI Conference on Artificial Intelligence*.

Claire Bonial, L. Donatelli, Mitchell Abrams, Stephanie M. Lukin, Stephen Tratz, Matthew Marge, Ron Artstein, David R. Traum, and Clare R. Voss. 2020. Dialogue-amr: Abstract meaning representation for dialogue. In *LREC*.

Deng Cai and Wai Lam. 2020. AMR parsing via graph-sequence iterative inference. In *Proceedings of the 58th Annual Meeting of the Association for Computational Linguistics*, pages 1290–1301, Online. Association for Computational Linguistics.

Shu Cai and Kevin Knight. 2013. Smatch: an evaluation metric for semantic feature structures. In *Proceedings of the 51st Annual Meeting of the Association for Computational Linguistics (Volume 2: Short Papers)*, pages 748–752, Sofia, Bulgaria. Association for Computational Linguistics.

Liang Chen, Peiyi Wang, Runxin Xu, Tianyu Liu, Zhifang Sui, and Baobao Chang. 2022. ATP: AMRize then parse! enhancing AMR parsing with PseudoAMRs. In *Findings of the Association for Computational Linguistics: NAACL 2022*, pages 2482–2496, Seattle, United States. Association for Computational Linguistics.

Ziming Cheng, Z. Li, and Hai Zhao. 2022. Bibl: Amr parsing and generation with bidirectional bayesian learning. In *International Conference on Computational Linguistics*.

Marco Damonte, Shay B. Cohen, and Giorgio Satta. 2017. An incremental parser for Abstract Meaning Representation. In *Proceedings of the 15th Conference of the European Chapter of the Association for Computational Linguistics: Volume 1, Long Papers*, pages 536–546, Valencia, Spain. Association for Computational Linguistics.

Ramón Fernandez Astudillo, Miguel Ballesteros, Tahira Naseem, Austin Blodgett, and Radu Florian. 2020. Transition-based parsing with stack-transformers. In *Findings of the Association for Computational Linguistics: EMNLP 2020*, pages 1001–1007, Online. Association for Computational Linguistics.

Jeffrey Flanigan, Sam Thomson, Jaime Carbonell, Chris Dyer, and Noah A. Smith. 2014. A discriminative graph-based parser for the Abstract Meaning Representation. In *Proceedings of the 52nd Annual Meeting of the Association for Computational Linguistics (Volume 1: Long Papers)*, pages 1426–1436, Baltimore, Maryland. Association for Computational Linguistics.

DongLai Ge, Junhui Li, Muhua Zhu, and Shoushan Li. 2019. Modeling source syntax and semantics for neural amr parsing. In *IJCAI*, pages 4975–4981.

Hardy Hardy and Andreas Vlachos. 2018. Guided neural language generation for abstractive summarization using abstract meaning representation. In *Proceedings of the 2018 Conference on Empirical Methods in Natural Language Processing*, pages 768–773.

Ching-Kang Ing. 2007. Accumulated prediction errors, information criteria and optimal forecasting for autoregressive time series.

Young-Suk Lee, Ramón Fernandez Astudillo, Tahira Naseem, Revanth Gangi Reddy, Radu Florian, and Salim Roukos. 2020. Pushing the limits of amr parsing with self-learning. In *Proceedings of the 2020 Conference on Empirical Methods in Natural Language Processing: Findings*, pages 3208–3214.

Mike Lewis, Yinhan Liu, Naman Goyal, Marjan Ghazvininejad, Abdelrahman Mohamed, Omer Levy, Veselin Stoyanov, and Luke Zettlemoyer. 2020. BART: Denoising sequence-to-sequence pre-training

for natural language generation, translation, and comprehension. In *Proceedings of the 58th Annual Meeting of the Association for Computational Linguistics*, pages 7871–7880, Online. Association for Computational Linguistics.

Kexin Liao, Logan Lebanoff, and Fei Liu. 2018. Abstract meaning representation for multi-document summarization. In *Proceedings of the 27th International Conference on Computational Linguistics*, pages 1178–1190.

Yijin Liu, Fandong Meng, Yufeng Chen, Jinan Xu, and Jie Zhou. 2021. Scheduled sampling based on decoding steps for neural machine translation. In *Proceedings of the 2021 Conference on Empirical Methods in Natural Language Processing, EMNLP 2021, Virtual Event / Punta Cana, Dominican Republic, 7-11 November, 2021*, pages 3285–3296. Association for Computational Linguistics.

Chunchuan Lyu and Ivan Titov. 2018. AMR parsing as graph prediction with latent alignment. In *Proceedings of the 56th Annual Meeting of the Association for Computational Linguistics (Volume 1: Long Papers)*, pages 397–407, Melbourne, Australia. Association for Computational Linguistics.

Arindam Mitra and Chitta Baral. 2016. Addressing a question answering challenge by combining statistical methods with inductive rule learning and reasoning. In *Proceedings of the AAAI Conference on Artificial Intelligence*, volume 30.

Tahira Naseem, Abhishek Shah, Hui Wan, Radu Florian, Salim Roukos, and Miguel Ballesteros. 2019. Rewarding smatch: Transition-based amr parsing with reinforcement learning. *arXiv preprint arXiv:1905.13370*.

Sudha Rao, Daniel Marcu, Kevin Knight, and Hal Daumé III. 2017. Biomedical event extraction using abstract meaning representation. In *BioNLP 2017*, pages 126–135.

Mrinmaya Sachan and Eric Xing. 2016. Machine comprehension using rich semantic representations. In *Proceedings of the 54th Annual Meeting of the Association for Computational Linguistics (Volume 2: Short Papers)*, pages 486–492.

Peiyi Wang, Liang Chen, Tianyu Liu, Baobao Chang, and Zhifang Sui. 2021. Hierarchical curriculum learning for amr parsing. In *Annual Meeting of the Association for Computational Linguistics*.

Yanshan Wang, Sijia Liu, Majid Rastegar-Mojarad, Liwei Wang, Feichen Shen, Fei Liu, and Hongfang Liu. 2017. Dependency and amr embeddings for drug-drug interaction extraction from biomedical literature. In *Proceedings of the 8th acm international conference on bioinformatics, computational biology, and health informatics*, pages 36–43.

Ledell Wu, Fabio Petroni, Martin Josifoski, Sebastian Riedel, and Luke Zettlemoyer. 2019. Scalable zero-shot entity linking with dense entity retrieval. *arXiv preprint arXiv:1911.03814*.

Benfeng Xu, Licheng Zhang, Zhendong Mao, Quan Wang, Hongtao Xie, and Yongdong Zhang. 2020a. Curriculum learning for natural language understanding. In *Proceedings of the 58th Annual Meeting of the Association for Computational Linguistics*, pages 6095–6104, Online. Association for Computational Linguistics.

Dongqin Xu, Junhui Li, Muhua Zhu, Min Zhang, and Guodong Zhou. 2020b. Improving amr parsing with sequence-to-sequence pre-training. In *Proceedings of the 2020 Conference on Empirical Methods in Natural Language Processing (EMNLP)*, pages 2501–2511.

Runxin Xu, Peiyi Wang, Tianyu Liu, Shuang Zeng, Baobao Chang, and Zhifang Sui. 2022. A two-stream amr-enhanced model for document-level event argument extraction. In *North American Chapter of the Association for Computational Linguistics*.

Chen Yu and Daniel Gildea. 2022a. Sequence-to-sequence AMR parsing with ancestor information. In *Proceedings of the 60th Annual Meeting of the Association for Computational Linguistics (Volume 2: Short Papers)*, pages 571–577, Dublin, Ireland. Association for Computational Linguistics.

Chenyao Yu and Daniel Gildea. 2022b. Sequence-to-sequence amr parsing with ancestor information. In *Annual Meeting of the Association for Computational Linguistics*.

Sheng Zhang, Xutai Ma, Kevin Duh, and Benjamin Van Durme. 2019a. AMR parsing as sequence-to-graph transduction. In *Proceedings of the 57th Annual Meeting of the Association for Computational Linguistics*, pages 80–94, Florence, Italy. Association for Computational Linguistics.

Sheng Zhang, Xutai Ma, Kevin Duh, and Benjamin Van Durme. 2019b. Broad-coverage semantic parsing as transduction. In *Proceedings of the 2019 Conference on Empirical Methods in Natural Language Processing and the 9th International Joint Conference on Natural Language Processing (EMNLP-IJCNLP)*, pages 3786–3798, Hong Kong, China. Association for Computational Linguistics.

Wen Zhang, Yang Feng, Fandong Meng, Di You, and Qun Liu. 2019c. Bridging the gap between training and inference for neural machine translation. In *Proceedings of the 57th Annual Meeting of the Association for Computational Linguistics*, pages 4334–4343, Florence, Italy. Association for Computational Linguistics.

Zixuan Zhang and Heng Ji. 2021. Abstract meaning representation guided graph encoding and decoding for joint information extraction. In *Proceedings of*

the 2021 Conference of the North American Chapter of the Association for Computational Linguistics: Human Language Technologies, pages 39–49.

Jiawei Zhou, Tahira Naseem, Ramón Fernandez Astudillo, and Radu Florian. 2021. AMR parsing with action-pointer transformer. In *Proceedings of the 2021 Conference of the North American Chapter of the Association for Computational Linguistics: Human Language Technologies*, pages 5585–5598, Online. Association for Computational Linguistics.

Qiji Zhou, Yue Zhang, Donghong Ji, and Hao Tang. 2020. AMR parsing with latent structural information. In *Proceedings of the 58th Annual Meeting of the Association for Computational Linguistics*, pages 4306–4319, Online. Association for Computational Linguistics.

A Training Configuration

AMR Parsing on AMR 2.0/3.0	
Model Name	AMRBART (Bai et al., 2022)
Pretrained Model	AMRBART-Large
Learning Rate	8e-6
Batchsize	16
Accumulation Steps	4
Max Epochs	30
Validation Interval	1 epoch
Early Stopping	10
Beam size	5
Warmup Steps	200
Entity Linking	BLINK (Wu et al., 2019)

Table 5: The Hyper-Parameters for all of our implemented models including RGL and baseline models.

We use hyper-parameters shown in table 5 to train all of our implemented models, including the baseline and R2L parser for inference. Before training the RGL, we use the state dict of the encoder of AMRBART to initialize the graph encoder and then train the model using the same configuration. As for the R2L parser for training, we random select a part of the training set in the ratio of 0.3, then we use these gold labeled data to train the R2L parser.

We implemented our models on the Pytorch framework. All the models are trained on a single NVIDIA Tesla A100 GPU. Training takes 17 hours on AMR 2.0 and 24 hours on AMR 3.0.

B Detailed Evaluation Metrics

We use the Smatch scores (Cai and Knight, 2013) to evaluate the performance. The further the break down scores (Damonte et al., 2017) is shown as follows. i) No WSD, compute while ignoring Propbank senses (e.g., duck-01 vs duck-02), ii) Wikification, F-score on the wikification (:wiki roles), iii) Concepts, F-score on the concept identification task, iv) NER, F-score on the named entity recognition (:name roles), v) Negations, F-score on the negation detection (:polarity roles), vi) Unlabel, compute on the predicted graphs after removing all edge labels, vii) Reentrancy, computed on reentrant edges only, viii) Semantic Role Labeling (SRL), computed on :ARG-i roles only.

C Case Study

The illustrated example in figure 9 shows the accumulation of structural loss more intuitively. We align the variables predicted by the model with the standard AMR graph and mark the prediction errors in red. From the figure, we can see that there are more errors in the later part of the predicted AMR graph. What's more, the relation ":snt2" is wrongly predicted due to the error of the previous relations ":op1" and ":op2", which shows that the duplicate dependencies imposed by sequence-to-sequence manner on AMR parsing have an negative effect.

Sentence

There are many who have a sense of urgency, quietly watching how things develop,you are dragons coiling, you are tigers crouching, I admire noble-minded patriots.

AMR graph

```
(m / multi-sentence
    :snt1 (m2 / many
        :ARG0-of (s / sense-01
            :ARG1 (u / urgency)
            :time (w / watch-01
                :ARG0 m2
                :ARG1 (t3 / thing
                    :manner-of (d / develop-02
                        :ARG0 (t / thing)))
                :manner (q / quiet-04
                    :ARG1 m2))))
    :snt2 (d2 / dragon
        :domain (y / you)
        :ARG0-of (c / coil-01))
    :snt3 (t2 / tiger
        :domain (y2 / you)
        :ARG0-of (c2 / crouch-01))
    :snt4 (a / admire-01
        :ARG0 (i / i)
        :ARG1 (p / patriot
            :ARG0-of (m3 / mind-04
                :mod (n / noble)))))
```

AMR graph predicted by AMRBART

```
(m / multi-sentence
    :snt1 (m2 / many
        :ARG0-of (s / sense-01
            :mod (u / urgency)
            :time (w / watch-01
                :ARG0 m2
                :ARG1 (t3 / thing
                    :manner-of (d / develop-02
                        ~~:ARG0 (t / thing)~~))
                :manner (q / quiet-04
                    :ARG1 m2))))
    :op1 (d2 / dragon
        :ARG0 (y / you)
        :ARG0-of (c / coil-01))
    :op2 (t2 / tiger
        :ARG0 (y2 / you)
        :ARG0-of (c2 / crouch-01))
    :snt2 (a / admire-01
        :ARG0 (i / i)
        :ARG1 (p / patriot
            ~~:ARG0-of (m3 / mind-04~~
                ~~:mod (n / noble)~~))))
```

Figure 9: An example of AMR parsing of the long sentence from the validation set of AMR 3.0.